



***Sargassum wightii* Extract as a Green Inhibitor for Corrosion of Brass in 0.1 N Phosphoric Acid Solution**

R. SELVA KUMAR^{12*} and V. CHANDRASEKARAN³

¹Department of Chemistry, Research Scholar (PT), Bharathiar University, Coimbatore - 641 046, India.

²Department of Chemistry, Sree Krishna Polytechnic College, Nagercoil - 629 003, India.

³Department of Chemistry, Govt. Arts College (Autonomous), Salem – 636 007 India.

*Corresponding author E-mail: rselvakumar86@yahoo.com

<http://dx.doi.org/10.13005/ojc/310239>

(Received: April 15, 2015; Accepted: May 13, 2015)

ABSTRACT

The effect of marine algae *Sargassum wightii* extract on corrosion inhibition of brass in phosphoric acid was investigated by weight-loss method, potentiodynamic polarization and electrochemical impedance spectroscopy studies. The inhibition efficiency is found to increase with increasing concentration of extract and decreases with rise in temperature. The inhibitive effect could be attributed to the phytochemical constituents present in the inhibitor containing N, S, O atoms. The activation energy, thermodynamic parameters (free energy, enthalpy and entropy change) and kinetic parameters (rate constant and half-life) for inhibition process were calculated. These thermodynamic and kinetic parameters indicate a strong interaction between the inhibitor and the brass surface. The inhibition is assumed to occur via adsorption of inhibitor molecules on the brass surface, which obeys Temkin adsorption isotherm. The adsorption of inhibitor on the brass surface is exothermic, physical, and spontaneous, follows first order kinetics. The polarization measurements showed that the inhibitor behaves as a mixed type inhibitor. Inhibition efficiency values were found to show good trend with weight-loss method, potentiodynamic polarization and electrochemical impedance spectroscopy studies. Surface study techniques (FT-IR and SEM) were carried out to ascertain the inhibitive nature of the algal extract on the brass surface.

Key words: Brass, Phosphoric acid, *Sargassum wightii*, Inhibition, Polarization, Isotherm.

INTRODUCTION

Phosphoric acid (H_3PO_4) is a major chemical product, which has many important uses especially in the production of fertilizers. Most of the acid is produced from phosphate rock by wet process. Brass and stainless steel are frequently used in many parts of the wet process and a

considerable quantity of data has been published about the resistance of these materials to corrosion by acid solutions^{1,2}. Most of the previous studies were focused on the inhibition of metals in HCl or H_2SO_4 solutions using organic compounds containing N, S, O atoms as corrosion inhibitors³⁻⁵. A lot of research has been done with naturally occurring substances since they are known to be

eco-friendly and with little or no side effect on the humans. Among the naturally occurring substances reported in the corrosion study of metals like brass, aluminium, tin and mild steel, there leave extracts, gums and exudates, dyes, oils from plant materials, plant seeds and fruits, and anti-bacterial drugs. Plant extracts like the extract of *Cocos nucifera*-coconut palm-petiole⁶; *Musa Paradisiaca*⁷; *Mentha Pulegium*⁸; *Treculia Africana* leaves⁹ and *Lupinus varius* leaves¹⁰ have been studied and established their corrosion inhibition effects. They were all found to be good corrosion inhibitors with no effect on the environment.

In the present study, the effect of addition of marine algae *Sargassum wightii* extract on corrosion inhibition of brass in 0.1 N phosphoric acid solutions at different temperatures and various time intervals have been investigated by weight-loss method, potentiodynamic polarization and electrochemical impedance spectroscopy studies. The weight loss measurements aimed to predict the inhibition efficiency on brass corrosion and the adsorption isotherm, thermodynamic and kinetic feasibility of inhibition *via* surface coverage on brass by adsorbed SWE. The inhibition type and inhibition efficiency were determined from the polarization measurements and impedance spectroscopy studies. Surface analytical techniques (FT-IR and SEM) were carried out to ascertain the inhibitive nature of the algal extract on the brass surface.

MATERIAL AND METHODS

Materials

The chemical composition (weight percent) of the brass used in the present study was 71.5 % Cu, 28.38 % Zn, 0.07 % Pb, and 0.05 % Fe. The geometry of the specimens for weight-loss experiments was as follows: The brass specimens were polished mechanically with different grades of emery papers (1/0 to 4/0) and were thoroughly washed with double distilled water then degreased in acetone and dried. The solutions were prepared from analar grade chemicals using double distilled water. Phosphoric acid solution (H_3PO_4) was used as a corrosion medium. The inhibitor *Sargassum wightii* extract (SWE) was extracted with ethanol using soxhelt extractor from marine algae *Sargassum wightii*.

The chemical structure of some active compounds separated¹¹ from *Sargassum wightii* are shown in Scheme-1.

Weight-loss study

Measurements of weight changes were performed with rectangular brass specimens (length: 5 cm, width: 1 cm, and thickness: 0.3 cm). The specimens with same dimensions were immersed in 100 ml of 0.1 N H_3PO_4 solutions with and without different concentrations (0.0001 % to 0.0005 %) of SWE and allowed stand for 3 h and 6 h at various temperatures were as follows: 300 K, 318 K, 328 K, and 338 K. At 300 K the specimens were immersed for immersion time of 24, 48, 72, and 96 h. Then, the specimens were rinsed with distilled water and adherent corrosion products for 20 s. Then, the specimens were rinsed with water, cleaned with acetone and dried. The percentage of inhibition efficiency (IE) over the exposure period was calculated using the following equation (1)¹²:

$$IE (\%) = \frac{W_o - W_i}{W_o} \times 100 \quad \dots(1)$$

where W_o and W_i are the rate of corrosion for brass with and without inhibitor, respectively.

Potentiodynamic polarization studies

The potentiodynamic polarization studies were carried out with brass strips having an exposed area of 1 cm². The cell assembly consisted of brass as working electrode, a platinum foil as counter electrode and a saturated calomel electrode as a reference electrode. Polarization studies were carried out using a potentiostat/galvanostat (Model BAS-100A) at 300 K. The working electrode was immersed in a 0.1 N H_3PO_4 and allowed to stabilize for 30 min. Each electrode was immersed in a 0.1 N H_3PO_4 in the presence and absence of different concentrations of inhibitor to which a current of 1.5 mA/cm² was applied for 20 minutes to reduce oxides. The cathodic and anodic polarization curves for brass specimen in the test solution with and without various concentrations of the inhibitor were recorded by scanning the potential range +200 from the corrosion potential at a sweep rate of 1 mV/s. The inhibition efficiencies were determined from corrosion currents using the Tafel extrapolation

method. The corrosion inhibition efficiency (IE) was calculated from the following equation (2):

$$IE (\%) = \frac{i_{\text{corr}} - i_{\text{corr}(i)}}{i_{\text{corr}}} \times 100 \quad \dots(2)$$

where i_{corr} and $i_{\text{corr}(i)}$ are the corrosion current density values without and with inhibitor, respectively.

Electrochemical impedance spectroscopy studies

The electrochemical impedance spectroscopy measurements are carried out with well polished brass electrode introduced into 100 ml of test solution using a Solartron electrochemical measurement unit (1280B). After the determination of the steady-state current at a corrosion potential, sine wave voltage (10 mV) peak to peak, at frequencies between 10 MHz and 10 KHz are superimposed on the rest potential. Computer programs automatically controlled the measurements performed at rest potential after 30 minutes of exposure at 300 K. The impedance diagrams are given in the Nyquist representation. From the Nyquist plot, the charge transfer resistance (R_{ct}) and double layer capacitance (C_{dl}) values were calculated.

The charge transfer resistance values were obtained from the plots of Z' vs Z'' . The values of ($R_s + R_{ct}$) correspond to the point where the plots cuts Z' axis at low frequency and R_s corresponds to the point where the plot cuts Z' axis at high frequency. The difference between R_{ct} and R_s values give the charge transfer resistance (R_{ct}) values. The C_{dl} values were obtained from the following equation (3):

$$C_{dl} = \frac{1}{2\pi f_{\text{max}} \times R_{ct}} \quad \dots(3)$$

where C_{dl} is double layer capacitance, R_{ct} is charge transfer resistance and f_{max} is frequency at $Z\Delta$ value maximum.

The inhibition efficiency (IE %) from the electrochemical impedance measurement was calculated using the following equation (4):

$$IE(\%) = \frac{R_{ct(i)} - R_{ct}}{R_{ct(i)}} \times 100 \quad \dots(4)$$

where R_{ct} and $R_{ct(i)}$ are the charge transfer resistance in the absence and presence of inhibitor respectively.

Surface study

The brass specimen was immersed in 0.1 N H_3PO_4 in the presence of inhibitor for 6 h at 300 K. After 6 h the specimen was taken out and dried. The nature of the film formed on the brass surface was analyzed by FT-IR Perkin Elmer-1600 spectrometer. SEM images were recorded with a Hitachi 3000H Microscope from the dried film formed on the surface of the brass specimens taken from 0.1 N H_3PO_4 in the presence and absence of inhibitor immersed for 6 h at 300 K.

RESULTS AND DISCUSSION

Weigh-loss method

Table-1 shows the inhibition efficiency values of brass by weight-loss measurements at different inhibitor concentrations of SWE in 0.1 N H_3PO_4 for different immersion times and temperatures. It has been observed that the inhibition efficiency increases with increase in concentration of inhibitor and decreases with increase in temperature and immersion time. The maximum IE (94.74 %) of inhibitor was achieved at 0.0005 % of inhibitor at 300 K for 3 h. This result suggests that an increase in extract concentration increases the number of inhibitor molecules absorbed onto the brass surface and reduces the surface area that is available for the direct acid attack on the metal surface⁶.

Thermodynamic and kinetic analysis

The adsorption of the organic compounds can be described by two main types of interactions: physical adsorption and chemisorptions. They are influenced by the nature of the charge of the metal, the chemical structure of the inhibitor, pH, the type of the electrolyte and temperature⁶.

Activation energy

In order to elucidate the inhibitive

properties of the inhibitor and the temperature dependence on the corrosion rates, the energy of activation for the corrosion process in the absence and presence of the inhibitor was evaluated from the following Arrhenius equation (5)¹³ and the values obtained are presented in Table-2:

$$\log \frac{p_2}{p_1} = \frac{E_a}{2.303 \times R} \left[\frac{1}{T_1} - \frac{1}{T_2} \right] \quad \dots(5)$$

where p_1 and p_2 are rate of corrosion at temperatures T_1 and T_2 respectively.

Arrhenius plot for the corrosion rate of brass in the presence SWE for 3 h and 6 h are given in Figure 1: (a)-(b). Straight lines were obtained from the plot of Log P versus $1/T$ with slope equal to $-E_a / 2.303 R$. Note first that the E_a values are low, indicating fast corrosion of brass in both the solutions¹⁴. The estimated values of E_a for brass corrosion in 0.1 N H_3PO_4 in the presence of SWE are listed in the Table -2. The values of $E_a > 80$ KJ/mol indicate chemical adsorption where as $E_a < 80$ KJ/mol infer physical adsorption. The E_a values indicate that the process is activation controlled. In the present study, the E_a values support the fact that the inhibitors are physically adsorbed on brass surface. The estimated E_a in the presence of inhibitor

Table 1: Calculated inhibition efficiency (IE) and surface coverage (SC) values for SWE on brass corrosion in 0.1 N H_3PO_4 for different immersion temperatures and times

Conc. of inhibitor (%)	For 3 h		For 6 h		At 300 K	
	SC(θ)	IE(%)	SC(θ)	IE(%)	SC(θ)	IE(%)
		At 300 K			24 h	
0.0000	0	0	0	0	0	0
0.0001	0.5790	57.90	0.2692	26.92	0.3636	36.36
0.0002	0.6316	63.16	0.3462	34.62	0.3896	38.96
0.0003	0.6842	68.42	0.3846	38.46	0.4286	42.86
0.0004	0.8421	84.21	0.5000	50.00	0.4805	48.05
0.0005	0.9474	94.74	0.6539	65.39	0.5455	54.55
		At 318 K			For 48 h	
Blank	0	0	0	0	0	0
0.0001	0.5238	52.38	0.2121	21.21	0.2528	25.28
0.0002	0.5714	57.14	0.2727	27.27	0.2697	26.97
0.0003	0.6667	66.67	0.3636	36.36	0.2865	28.65
0.0004	0.7143	71.43	0.4546	45.46	0.3371	33.71
0.0005	0.7619	76.19	0.5758	57.58	0.4157	41.57
		At 328 K			For 72 h	
Blank	0	0	0	0	0	0
0.0001	0.4167	41.67	0.1786	17.86	0.2110	21.10
0.0002	0.4583	45.83	0.2321	23.21	0.2363	23.63
0.0003	0.5833	58.33	0.2679	26.79	0.2490	24.90
0.0004	0.6667	66.67	0.3036	30.36	0.2954	29.54
0.0005	0.7083	70.83	0.4107	41.07	0.3544	35.44
		At 338 K			For 96 h	
Blank	0	0	0	0	0	0
0.0001	0.2647	26.47	0.1493	14.93	0.1581	15.81
0.0002	0.3235	32.35	0.1791	17.91	0.1733	17.33
0.0003	0.4412	44.12	0.2239	22.39	0.1854	18.54
0.0004	0.5588	55.88	0.2836	28.36	0.2188	21.88
0.0005	0.6177	61.77	0.3881	38.81	0.2736	27.36

Table 2: Calculated activation energy (E_a), free energy of adsorption (ΔG_{ads}), enthalpy change (ΔH), entropy change (ΔS) values for SWE on brass corrosion in 0.1 N H_3PO_4 at 300 K

Conc. of inhibitor (%)	E_a from equation (kJ/mol)	E_a from Arrhenius Plot (kJ/mol)	ΔG_{ads} (kJ/mol)	ΔH (kJ/mol)	ΔS (mol/kJ)
For 3 h					
Blank	12.91	12.98	0	0	0
0.0001	25.28	16.51	-29.47	-24.78	0.0156
0.0002	26.39	27.35	-27.62	-24.67	0.0098
0.0003	25.58	31.92	-26.43	-24.62	0.0060
0.0004	35.72	35.49	-24.50	-24.59	0.0028
0.0005	56.94	42.55	-21.50	-24.52	0.0005
For 6 h					
Blank	21.00	16.76	0	0	0
0.0001	24.38	22.53	-28.94	-24.72	0.0141
0.0002	26.05	23.94	-27.56	-24.70	0.0095
0.0003	26.15	27.36	-26.66	-24.67	0.0066
0.0004	28.98	28.72	-26.08	-24.66	0.0047
0.0005	33.65	34.19	-25.27	-24.60	0.0022

Table 3: Calculated rate constant (k) and half-life period ($t_{1/2}$) values for SWE on brass corrosion in 0.1 N H_3PO_4 at 300 K

Conc. of inhibitor (%)	Half-life Period(sec)	Rate constant (sec^{-1})
0.0001	1.2037	0.5758
0.0002	1.2037	0.5758
0.0003	1.1368	0.6096
0.0004	1.1178	0.6200
0.0005	1.1035	0.6280

infer that the interaction between the metal surface and the inhibitor was found to be strong enough to reduce corrosion¹⁴. The E_a values increases in the presence of SWE is often interpreted as physical adsorption with the formation of an adsorptive film with an electrostatic character¹³. In addition, the E_a values increases in the same order as the inhibition efficiency. This indicates that the energy barrier for the corrosion reaction increases in the presence of inhibitor in the acid solutions, the corrosion reaction will be further pushed to surface sites that are characterized by higher values of E_a indicating that

Table 4: Electrochemical parameters and inhibition efficiency (IE) for corrosion of brass in 0.1 N H_3PO_4 containing different concentrations of SWE

Conc. of inhibitor (%)	OCP (mV)	E_{corr} (mV)	Tafel constants		i_{corr} (mA/cm ²)	IE (%)
	vs. SCE	vs. SCE	b_a (mV/dec)	b_c (mV/dec)		
Blank	-193	-190	300	100	310	0
0.0001	-210	-190	270	100	210	32.26
0.0002	-230	-230	140	170	180	41.91
0.0003	-235	-240	60	90	160	48.39
0.0004	-240	-240	40	130	98	69.00
0.0005	-244	-250	38	150	63	92.00

corrosion occurs at the uncovered part of the surface¹⁵.

Free energy of adsorption

The free energy of adsorption ΔG_{ads} were obtained from the following equations and the values obtained are presented in Table-2:

$$\Delta G_{ads} = -RT \ln (55.5K) \quad \dots(6)$$

where K is given by

$$K = \frac{\theta}{C(1-\theta)} \quad \dots(7)$$

where θ is surface coverage on the metal surface, C is the concentration of inhibitor in mol/l, and K is equilibrium constant.

Results obtained indicate that the values of ΔG_{ads} are negative in all cases, indicating that the SWE extract is strongly adsorbed on the brass surface¹⁵. The value of ΔG_{ads} indicates that the inhibitor functions by physically adsorbing on the

surface of the brass. Generally values of ΔG_{ads} upto the $-29.47 \text{ KJmol}^{-1}$ are consistent with electrostatic interaction between charged molecules and a charged metal, while those more negative than the -40 KJmol^{-1} involve charge sharing or transfer from the inhibitor molecules to the metal surface to form a co-ordinate type of bond¹⁶. Physical adsorption is a result of electrostatic attraction between charged metal surface and charged species in the bulk of the solution. Adsorption of negatively charged species can also protect the positively charged metal surface acting with a negatively charged intermediate such as acid anions adsorbed on the metal surface⁶.

Entropy and enthalpy

Kinetic parameters such as enthalpy (ΔH) and entropy (ΔS) of activation of corrosion process is calculated from the following thermodynamic basic equations and the values obtained are presented in Table-2:

$$\Delta H = E_a - RT \quad \dots(8)$$

Table 5: AC Impedance parameters for corrosion of brass in 0.1 N H₃PO₄ containing different concentrations of SWE at 300 K

Conc. of inhibitor(%)	R _{ct} (ohm cm ²)	C _{dl} (mF/cm ²)	IE(%)
Blank	150.60	5.74	00.00
0.0001	407.10	2.71	63.00
0.0002	538.15	2.19	72.01
0.0003	630.42	1.98	76.11
0.0004	793.15	1.67	81.01
0.0005	2550.75	0.54	94.10

$$\Delta G_{ads} = \Delta H - T\Delta S \quad \dots(9)$$

Enthalpy of activation of absolute values lower than the $-24.78 \text{ KJmol}^{-1}$ indicates physical adsorption, and the values approaching 100 KJmol^{-1} indicate chemical adsorption¹⁰. In this study, the values of ΔH are lower than the $-24.78 \text{ KJmol}^{-1}$ confirming physical adsorption on the acid solutions. The negative values of ΔH also show that the adsorption of inhibitor is an exothermic process¹⁵. The ΔS values are positive for the acidic bath. This implies that the activation complex is the rate determining step representing association rather than

dissociation, indicating that a decrease in disorder takes place on going from reactant to the activated complex¹⁰.

Rate constant and half life

Figure 2: show the plots of $\log W_f$ (final weight loss) obtained in weight-loss studies vs. time in days for the brass dissolution. From the plots, the values of rate constant and half-life were evaluated using the following equations^{17,18} and the values obtained are presented in Table-3:

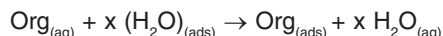
$$\text{Rate constant (k)} = 2.303 \times \text{slope (sec}^{-1}) \quad \dots(10)$$

$$\text{Half - life period } t_{1/2} = \frac{0.693}{k} (\text{sec}) \dots (11)$$

In this study, linear plots were obtained, which indicates first order kinetics⁹. In this study the rate constant values were decreased where as the half-life values were increased with increasing concentration of SWE.

Adsorption isotherms

The values of surface coverage r for different concentrations of the SWE at 300 K have been used to identify the best isotherm to determine the adsorption process. The adsorption of organic adsorbate on the surface of copper is regarded as substitutional process between the organic compound in the aqueous phase org_{aq} and the water molecules adsorbed on the copper surface $(\text{H}_2\text{O})_{\text{ads}}$ [19].



where x is the size ratio, that is the number of water molecules displaced by one molecule of organic inhibitor. Attempts were made to fit r values of various isotherms, including Langmuir, Freundlich, Temkin and Frumkin isotherms. By far the results were best fitted by Temkin adsorption isotherm. The Temkin adsorption isotherm is given by the following equation.

$$\ln kC = a0 \dots (12)$$

where k is the equilibrium constant of the adsorption reaction, C is the inhibitor concentration in the bulk of the solution and a is the molecule interaction parameters depending upon molecular interactions in the adsorption layer and the degree of heterogeneity of the metal surface. The plot of r against $\log C$ for all additives gives straight lines, as shown in Figure 3: (a)-(b). This indicates that these compounds are adsorbed on the surface of brass

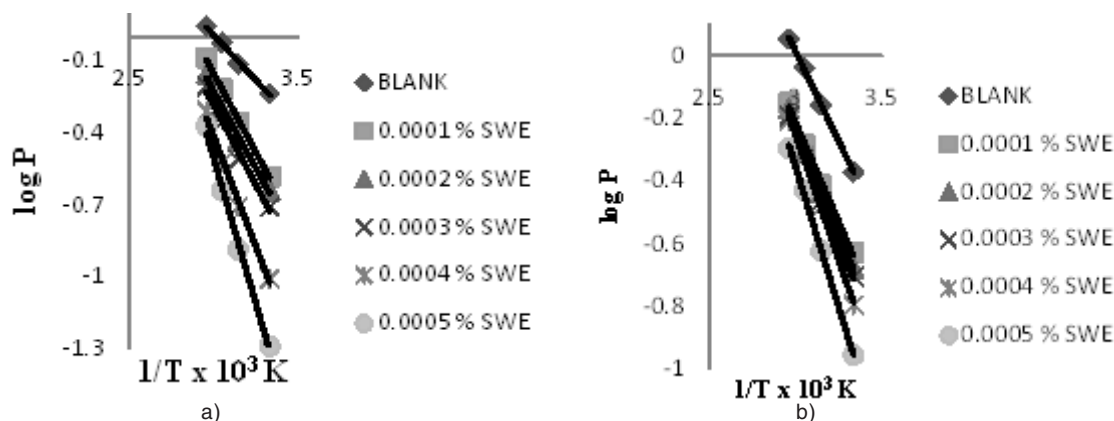


Fig. 1: Arrhenius plot for 0.1 N H₃PO₄ with different concentrations of SWE for different times

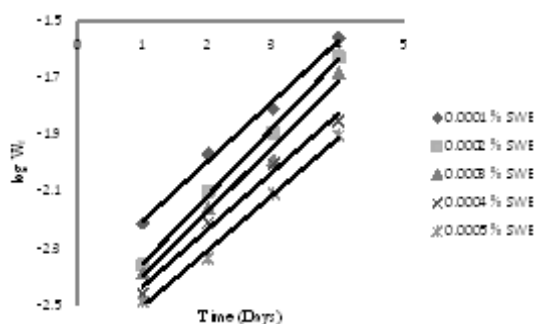


Fig. 2: Plot of $\log W_f$ vs. time (days) for 0.1 N H₃PO₄ with different concentrations of SWE

according to Temkin adsorption isotherm^{20,21}.

Potentiostatic polarization studies

Polarization measurement is an important research tool in the investigation of a variety of electrochemical phenomena. Such measurements permit studies of the reaction mechanism and the kinetics of corrosion phenomena on the metal deposition. Figure 4: shows the cathodic and anodic polarization curves of brass in 0.1 N H₃PO₄ with and without addition different concentrations of SWE. Table-4 gives the values of associated electrochemical parameters. The i_{corr} values

decreased with increasing concentration of inhibitor. The values of anodic Tafel slope (b_a) and cathodic Tafel slope (b_c) of SWE added solutions are found to change with inhibitor concentration, which clearly indicates that the inhibitors controlled both the anodic and cathodic reactions. Thus this inhibitor acted as a mixed type inhibitor [8]. The IE of SWE attained a maximum value at 0.0005 % concentration of inhibitor. The values of IE increased with increasing concentration of inhibitor, indicating that a higher surface coverage was obtained in solution with optimum concentration of inhibitor. The effect of the anodic polarization behavior of brass (Figure 4) suggests that protective films formed on the metal surface can alter anodic dissolution in solution shows that SWE formed a film that acted as

a barrier to protect the metal surface²⁰⁻²².

AC Impedance Measurements

AC impedance spectroscopy has been shown to be a powerful tool to study the corrosion process of metals in different environments and to characterize the inhibition ability of a corrosion inhibitor, which is related to the charge transfer resistance (R_{ct}). The double layer capacitance (C_{dl}) can also be used to determine the inhibition ability. The inhibition performance of an organic or natural substance on a metal surface depends not only on the chemical structure of the organic substance and the nature of the metal, but also on the experimental conditions such as the immersion time and

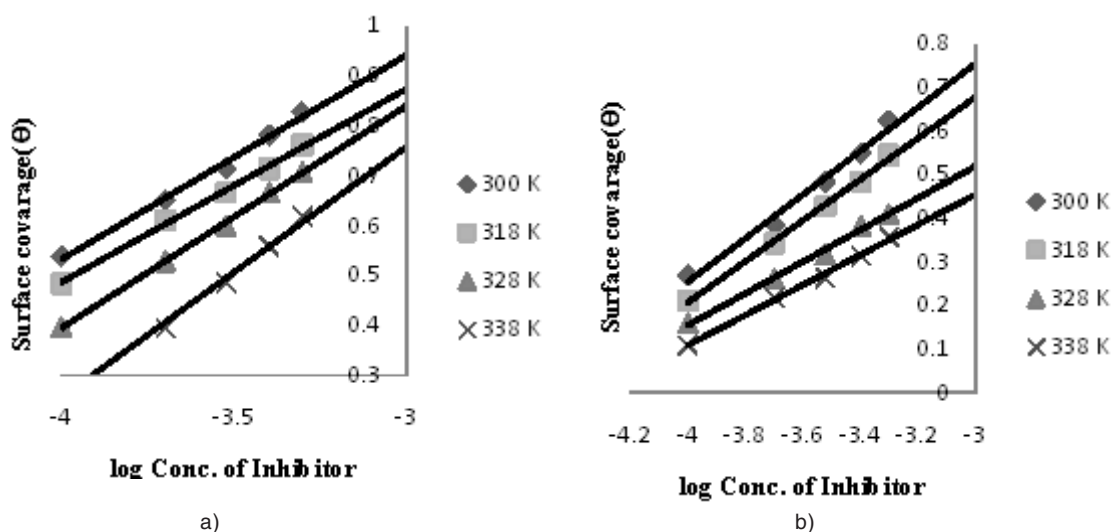


Fig. 3: Temkin's adsorption isotherm plot for 0.1 N H_3PO_4 with different concentrations of SWE for different times

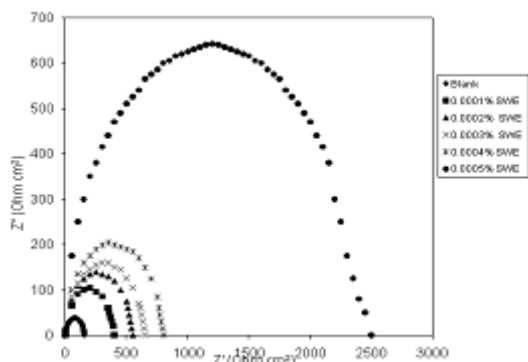


Fig. 5: Nyquist plots of brass in 0.1N H_3PO_4 with different concentrations of SWE

concentration of the adsorbent.

The corrosion behavior of brass, in acidic solution with and without SWE is also investigated by AC impedance measurements at 300 K (Figure 5). The impedance parameters and the IE % derived from the investigation are mentioned given in Table-5. As it can be seen from Figure 5, impedance diagrams show a semi-circular appearance, indicating that a charge transfer process mainly controls the corrosion of brass. From the impedance data, we notice an increase in the charge transfer resistance and decrease of the double layer capacitance with increasing the inhibitor

concentration, indicating that SWE inhibits the corrosion rate of brass by an adsorption mechanism. Therefore, the decrease in the C_{dl} value can be attributed to a decrease in the local dielectric constant and/or an increase in the thickness of the electrical double layer, suggesting that the inhibitor molecules act by adsorption at the metal/solution interface as a consequence of the replacement of water molecules by the inhibitor molecules⁸.

A comparison may be made between the inhibition efficiency values obtained by different methods (weight loss, potentiostatic polarization and AC impedance methods). We can see that whatever the method used, no significant changes are observed in IE % values. We can then conclude that there is a good agreement with the three methods used in this study at all tested concentrations and that the acid extract of *Sargassum wightii* acts as green inhibitor for acid corrosion of brass.

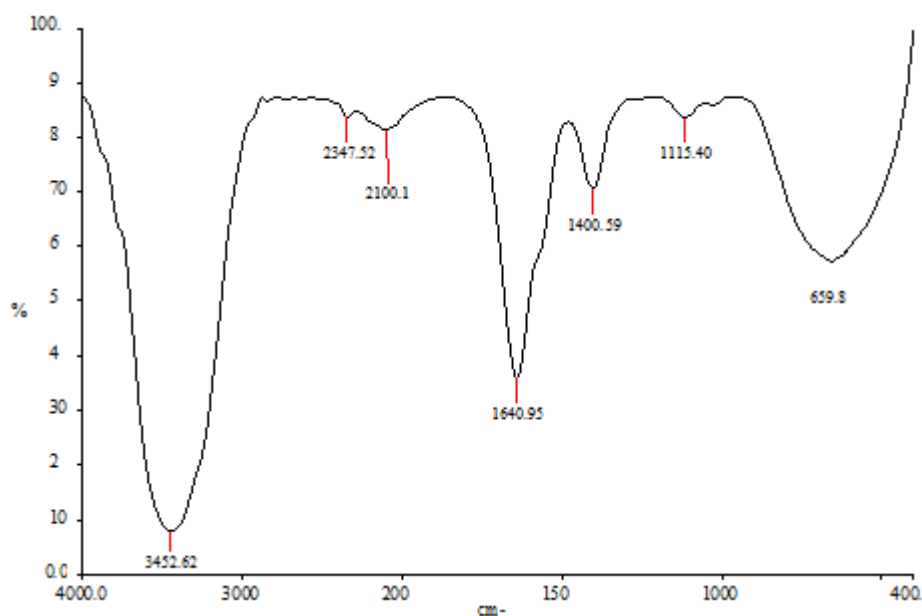


Fig. 6: FT-IR spectra of the surface of brass formed by immersing sample in 0.1 N H_3PO_4 with SWE for 6 h

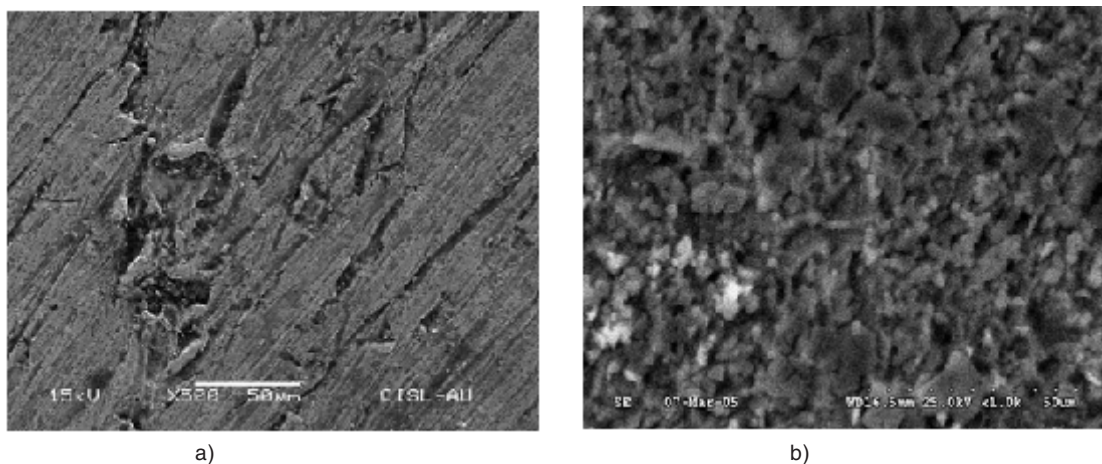


Fig. 7: SEM images of brass surface after 6 h immersion in 0.1N H_3PO_4 in the absence (a) and presence (b) of SWE

Surface examinations

FT-IR spectroscopy

The chemical analysis of *Sargassum wightii* found that many organic aromatic molecules, terpenoids, phenols, flavanoids, alkaloids, aromatic esters, benzyl alcohol, benzaldehyde and fatty acids are present in it²³. Figure 6: shows the FT-IR spectrum recorded in the range 400-4000 cm^{-1} to identify the functional groups present in SWE. From FT-IR, It was observed that aromatic molecules with following functional groups, intermolecular hydrogen bonding and O-H stretching (3452.62 cm^{-1}), $\text{-C}\equiv\text{N}$ in nitrile (2347.52 cm^{-1}), $\text{-C}\equiv\text{C}$ disubstituted alkyne (2100.13 cm^{-1}), -C-H and C=O stretching in aldehyde (1640.73 cm^{-1}), -C-H deformation in CH_3 (1400.59 cm^{-1}), -C-H stretching -C-O-C- (1115.40 cm^{-1}), and -C-H deformation in alkyne (659.86 cm^{-1}) are present in SWE. Further found that SWE inhibits the corrosion of brass specimen with high efficiency due to the presence of N and O in the organic molecules of SWE^{24,25}.

Scanning electron microscopy

SEM micrograms of the polished surface of brass exposed for 6 h in 0.1 N H_3PO_4 in absence and presence of SWE are shown in Figure 7: (a)-(b) shows the surface morphology of brass formed in 0.1 N H_3PO_4 without and with SWE for 6 h. In the comparison of the SEM micrograms, there were a rough surface on brass in absence of extract and a smooth surface with deposited extract in presence of the SWE. This confirms that the extract inhibited corrosion of brass through adsorption of the inhibitor molecules on metal surface. After immersing in the

inhibitor containing solution, the entire metal surface was covered with a layer formed with inhibitor as a barrier to corrosion, as denoted by rougher over abrasions. The inhibiting layer was possibly consisting of Cu^{2+} and Zn^{2+} complexes formed with the SWE derivatives are mentioned in FT-IR^{26,27}.

CONCLUSIONS

The inhibition efficiency of SWE on corrosion of brass in 0.1 N H_3PO_4 increases on increasing of concentration of the extract and decreases with rise in temperature. Adsorption of inhibitor molecules of the extract on brass surface is found to obey Tempkin adsorption isotherm. The increase in the values of activation energies of the corrosion process in the presence of extract indicates that SWE creates a physical barrier to charge and mass transfer, leading to reduction in corrosion rate of brass in 0.1 N H_3PO_4 . The negative values of ΔG_{ads} and ΔH highlight that the inhibition of corrosion of brass through adsorption is spontaneous and exothermic. Their values also reveal that physical adsorption is involved in the adsorption process. Potentiodynamic polarization measurements show that SWE acts as a mixed type inhibitor. Inhibition efficiency values were found to show good trend with weight-loss method, potentiodynamic polarization and electrochemical impedance spectroscopy studies. SEM and FT-IR studies confirm that corrosion inhibition of brass in 0.1 N H_3PO_4 is due to adsorption of the SWE extract on brass.

REFERENCES

1. Chandrasekaran, V.; Kannan, K.; Natesan, M. *Asian J. Chem.* **2005**, *17*(3), 1921-1934.
2. Chandrasekaran, V.; Kannan, K.; Natesan, M. *Orient. J. Chem.* **2005**, *21*(1), 81-88.
3. Ranjana ; Nandi, M. M. *Ind. J. Chem. Tech.* **2011**, *18*, 29-36.
4. Ranjana; Ranu Banerjee ; Nandi, M. M., *Ind. J. Chem. Tech.* **2013**, *20*, 237-244.
5. Ravichandran, R.; Rajendran, N. *App. Surf. Sci.* **2005**, *241*, 449-458.
6. Vijayalakshmi, P. R.; Rajalakshmi, R.; Subhashini, S. *Portu. Electrochim. Acta.* **2011**, *29*(1), 9-21.
7. Ramananda S. Mayanglambam; Vivek Sharma; Gurmeet Singh. *Portu. Electrochim. Acta.* **2011**, *29*(6), 405-417.
8. Khadraoui, A.; Khelifa, A.; Boutoumi, H.; Mettai, B.; Karzazi, Y.; Hammouti, B. *Portu. Electrochim. Acta.* **2014**, *32*(4), 271-280.
9. Ejikeme, P. M.; Umana, S. G.; Onukwuli, O. D.; Hammouti, B. *Portu. Electrochim. Acta.* **2012**, *30*(5), 317-328.
10. Muna K. Irshedat; Eyad M. Nawafleh; Tareq T. Bataineh; Riyadh Muhaidat; Mahmoud A. Al-Qudah; Ahmed A. Alomary; Hammouti, B. *Portu. Electrochim. Acta.* **2011**, *31*(1), 1-10.

11. Gao-Lei; Bo, L. Hammouti, B. *Portu. Electrochim. Acta.* **2014**, *28*, 735–752.
12. Ravichandran, R.; Rajendran, N. *App. Surf. Sci.* **2014**, *241*, 449-458.
13. Chandrasekaran, V.; Saravanan, J. *Corr. Sci. Tech.* **2006**, *5*(5), 160-167.
14. Mahmoud, S. S. *Portu. Electrochim. Acta.* **2006**, *24*, 441-455.
15. Elmsellem, H.; Basbas, N.; Chetouani, A.; Aouniti, A.; Radi, S.; Messali, M.; Hammouti B. *Portu. Electrochim. Acta.* **2014**, *32*(2), 77-108.
16. Tadeja Kosec; Ingrid Milosev; Boris Pihlar. *App. Surf. Sci.* **2007**, *253*, 8863-8873.
17. Chandrasekaran, V.; Kannan, K.; Natesan, M. *Corr. Sci. Tech.* **2005**, *4*(5), 191-200.
18. Al-Mhyawi, S. R. *Orient. J. Chem.*, **2014**, *30*(2), 541-552.
19. Megahed, H. E. *Portu. Electrochim. Acta.* **2011**, *29*(4), 287-294.
20. Chandrasekaran, V.; Gokulalakshmi, K. *Bull. Electrochem.* **2006**, *22*, 379-384.
21. Chandrasekaran, V.; Kannan, K.; Natesan, M. *Int. J. Pure and App. Chem.* **2006**, *1*(1), 101-115.
22. Gaikwad, A. B. ; Patil, P.P.; Sudeshna Chaudhari. *Curr. App. Phy.* **2009**, *9*, 206-218.
23. Dandelot, S.; Robles, C.; Pech, N.; Cazaubon, A. *Aqua. Bot.* **2008**, *88*(4), 311–316.
24. Ravichandran, R.; Nanjudan, S.; Rajendran, N. *App. Surf. Sci.*, **2004**, *236*, 241-250.
25. Du, X.S.; Su, Y.J. ; Li, J.X.; Qiao, L.J.; Chu, W.Y. *Corr. Sci.* **2012**, *60*, 69-75 .
26. Ramananda; Mayanglambam, S.; Vivek Sharma; Gurmeet Singh. *Portu. Electrochim. Acta.* **2011**, *29*(6), 405-417.
27. Khadraoui, A.; Khelifa, A.; Boutoumi, H.; Mettai, B.; Karzazi, Y.; Hammouti, B. *Portu. Electrochim. Acta.* **2014**, *32*(4), 271-280.